Journal of Sustainable Development Indicators

http://www.sdewes.org/jsdi

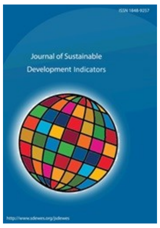

Year 2026, Volume 2, Issue 4, 1030777

Original Research Article

Development of Low-Cost Internet-of-Things Enabled Artificial Neural Network-Based Anaerobic Digester for Electricity Generation

Idowu A. Ayoade[1], **Michael I. Kayode**[2], **Omomunmi M. Longe**[1]*

[1]Department of Electrical and Electronics Engineering Science, University of Johannesburg, South Africa.

[2]Department of Mechatronics Engineering, First Technical University, Ibadan, Nigeria.

Corresponding Author e-mail: 224089150@student.uj.ac.za

Cite as: Ayoade, I. A., Kayode, M. I., Longe, O. M., Development of a Low-Cost Sensor-Based Monitoring and Artificial Neural Network Framework for Anaerobic Digester Electricity Generation, J. sustain. dev. indic., 2(4), 1030777, 2026, DOI: https://doi.org/10.13044/j.sdi.d3.0777

ABSTRACT

Off-grid electricity in energy-constrained communities can be supported by converting organic waste into biogas and electrical energy using affordable monitoring and predictive tools. This study developed an anaerobic digestion electricity-generation framework incorporating low-cost sensor-based monitoring and artificial neural network methane prediction. The modelling dataset comprised 61 daily records combining independently measured observations with controlled-profile augmentation across the investigated operating range. A wireless microcontroller-based sensing node monitored temperature and feedstock moisture, while temperature, biogas volume, carbon dioxide fraction, pH, hydrogen sulfide, and internal combustion engine operating time were used to predict methane. Methane output ranged from 6.50 to 12.09 cubic metres per day and daily electrical energy from 10.0 to 22.0 kilowatt-hours. On held-out test data, the neural network achieved a root mean square error of 0.593 cubic metres per day and a coefficient of determination of 0.856, whereas multiple linear regression achieved 0.416 and 0.929, respectively. The implied electrical conversion efficiency averaged 15.5%. The results demonstrate predictive feasibility within the investigated range, while the structured hybrid dataset and stronger linear baseline indicate that broader generalisation requires independently measured data under more variable operating conditions.

KEYWORDS

Anaerobic Digestion, Artificial Neural Network, Biogas, Electricity Generation, Sensor-Based Monitoring, Methane Prediction.

INTRODUCTION

Access to electricity in rural Africa remains a significant challenge, with a substantial portion of the population lacking reliable electricity. According to the International Energy Agency, as of 2019, only 38% of the population in rural Africa had access to electricity [1]. This issue is particularly critical in Sub-Saharan Africa, where less than 30% of the population has adequate access to electricity, owing to low electrification rates, poor infrastructure maintenance, and the fact that the majority reside in remote rural areas [2]. The situation is dire: approximately 620 million people in Africa lack access to electricity, equivalent to two-thirds of the continent's population [3]. Efforts to address rural electrification in Africa have been pursued through various means, including renewable energy sources such as wind power,

* Corresponding author

photovoltaic systems, and mini-grids. These initiatives aim to bridge the electricity access gap and accelerate development in Sub-Saharan Africa [4]. Decentralised systems, such as mini-grids, have been identified as crucial for increasing electricity access, especially in rural areas [5]. Studies have shown that community-based electric microgrids can significantly contribute to rural development by enhancing productivity, increasing income levels, and improving access to social and business services [6]. Despite this progress, approximately 600 million people in sub-Saharan Africa still lack access to electricity, with over 80% of them residing in rural areas [7]. This lack of access to clean energy is a significant issue that requires urgent attention to achieve the development goals by 2030 [8]. The disparities in electricity access between rural and urban communities in Africa highlight the need for innovative solutions and increased investment in rural electrification projects [9].

Grid extension to remote areas in Africa faces numerous challenges that hinder the provision of electricity in underserved regions. The terrain in rural zones often poses a significant obstacle, with rugged landscapes, dense jungles, and geographical remoteness making it impractical and costly to extend the grid [10]. The scattered settlement of consumers in these areas further complicates grid extension efforts, as households are dispersed over large areas, making it economically unviable to connect them to centralised grid infrastructure. Traditional electrification methods, such as grid extension and standalone diesel generators, have proven unsustainable in addressing the electrification challenges faced in sub-Saharan Africa. Governments often postpone grid extension projects in rural areas with scattered populations owing to technical and economic factors, further exacerbating the electricity access gap between urban and rural areas [11]. The high costs associated with grid electrification in areas with low population densities present a significant barrier to extending the grid to remote African regions [12]. In light of these challenges, alternative solutions, such as off-grid solar systems and mini-grids, have emerged as viable options for electrifying remote areas of Africa. Off-grid solar technologies have been identified as a preferable option for mass electrification in rural Africa, with grid infrastructure recommended to focus on selected prosperous regions [13]. Mini-grids, which offer decentralised electricity generation and distribution, have been recognised as a cost-effective and efficient means of providing electricity to areas with scattered households and low demand potential [14].

Decentralised electrification projects, including mini-grids and standalone photovoltaic systems, have gained traction in remote areas where grid extension is impractical [15]. These systems offer a reliable and sustainable source of electricity in regions where conventional grid electrification is unfeasible owing to technical, geographical, and environmental constraints [15]. By leveraging renewable energy sources and innovative technologies, such as hybrid energy systems, it is possible to overcome the challenges associated with grid extension to remote areas and improve electricity access in underserved communities by utilising organic waste resources in African communities, which play a significant role in waste management and can be valuable sources for energy production and environmental sustainability. Studies have highlighted the potential of organic waste, including food and livestock waste, as alternative energy sources for rural African households [16]. The conversion of organic waste into biogas through anaerobic digestion has been identified as an effective method for obtaining alternative energy sources in rural areas [17]. This approach addresses waste management challenges, contributes to reducing greenhouse gas emissions, and promotes sustainable energy practices in communities [18].

In rural African communities, organic waste, such as agricultural residues and household waste, can be used to produce biogas, compost, and organic fertilisers [19]. Implementing waste-to-energy projects that focus on recovering organic waste as biomethane and compost offers rural communities an opportunity to manage waste effectively while generating valuable resources. By harnessing the potential of organic waste, communities can reduce environmental pollution, improve soil fertility through composting, and enhance energy access through biogas production [17]. The availability of organic waste resources in African communities offers opportunities to develop green technologies and sustainable practices. Studies have emphasised the importance of unlocking the full potential of organic waste as a renewable energy resource through effective governance and waste management strategies [20]. By promoting the utilisation of organic waste for energy production, communities can reduce their reliance on fossil fuels, mitigate environmental impacts, and foster a culture of resource efficiency and conservation [21]. The rising global demand for sustainable energy solutions requires innovative approaches to waste management and renewable energy production. Anaerobic digestion provides a practical pathway for simultaneous organic-waste treatment and decentralised electricity generation. However, integration of affordable sensing, transparent methane-to-electricity accounting, predictive modelling, and supervisory decision support within small-scale systems remains limited. This study, therefore, develops an anaerobic digestion electricity-generation framework incorporating a low-cost sensor-based monitoring node and data-driven methane prediction.

The contribution lies in integrating process monitoring, unit-consistent energy accounting, explicit variable roles, predictive model benchmarking, and supervisory control logic within a single measurement-to-decision framework. Artificial neural network prediction is compared with multiple linear regression to determine whether nonlinear model complexity provides a measurable advantage. The control equations are presented as a supervisory design framework rather than experimentally validated closed-loop performance. Accordingly, novelty is attributed to the integrated and transparent framework rather than to neural-network prediction or low-cost sensing in isolation.

LITERATURE REVIEW OF ANAEROBIC DIGESTERS: BIOGAS GENERATION

Anaerobic digestion has been extensively investigated as a pathway for waste treatment, biogas production, and renewable-energy recovery. The study of [23] reviewed the fundamentals, operational challenges, and technological advances associated with anaerobic digestion. The results of [25] demonstrated that dynamic magnetic fields can enhance microbial electron-transfer processes associated with digestion performance. Steiniger et al. [36] examined the influence of digester temperature on process stability and related operating characteristics. The decentralised energy recovery through co-digestion of kitchen waste and blackwater [30]. The study [29] evaluated the electricity-generation potential of biogas produced by anaerobic digestion of vinasse. The assessment of [31] assessed enhanced digestion of agro-industrial waste from a life-cycle perspective. The review study of anaerobic digestion as a renewable biogas technology [32], while [33] compared environmental impacts and waste-to-energy efficiency for kitchen waste treatment. Jamaluddin and Zulkeflee [35] further demonstrated the relevance of low-cost biogas production for rural applications. Digital monitoring and predictive modelling have increasingly complemented conventional anaerobic digestion. The design in [28] developed a smart household biogas digester with integrated monitoring. While [24] examined the integration of artificial intelligence into anaerobic digestion to improve plant operation. The study in [26] applied artificial intelligence to condition-based maintenance of an anaerobic reactor. Thakur et al. [22] demonstrated the use of an artificial neural network to estimate calorific value, illustrating the potential of data-driven energy-property prediction. Lu et al. [34] investigated bioelectrocatalytic computation for the simultaneous treatment of digestate and biogas upgrading. Despite these developments, sensing, predictive modelling, supervisory control, and electricity-performance assessment are frequently addressed as separate functions. The present study combines these functions into a single small-scale framework and benchmarks the neural network model against a simpler linear alternative. This integrated measurement-to-decision structure constitutes the principal distinction of the study..

METHODS

This study investigates anaerobic digestion as a decentralised pathway for converting biodegradable waste into biogas and electrical energy. The overall digestion workflow is presented in Figure 1, while the principal biochemical conversion stages are summarised in Figure 2. The modelling dataset comprised 61 daily records combining independently measured observations with values generated through controlled-profile augmentation to represent intermediate and repeated operating conditions. Row-level provenance was not retained in the archived dataset; consequently, the observations were analysed jointly as a hybrid operational dataset. The structured ramp-up, plateau, and ramp-down profile can strengthen associations among variables and apparent predictive performance. Results are therefore interpreted within the represented operating envelope rather than as evidence of unrestricted model generalisability. Daily electricity values represent energy totals and are reported in kilowatt-hours. The methodological focus is on an integrated monitoring, control logic, and data-driven optimisation layer that supports stable operation and improved methane output. Operational data were collected as daily observations over 61 consecutive days (14 January 2024 to 14 March 2024) (Appendix 1). To resolve the reviewer's unit concern, all daily electricity values are treated as daily energy totals in kWh (not kWh/day); equivalently, "kWh/day" in the manuscript indicates "kWh per day (daily total)" and is therefore written as kWh throughout the revised text. The observed operating envelope, as represented in the dataset, is summarised in Table 1, and these variables form the basis for the statistical analysis and ANN modelling.

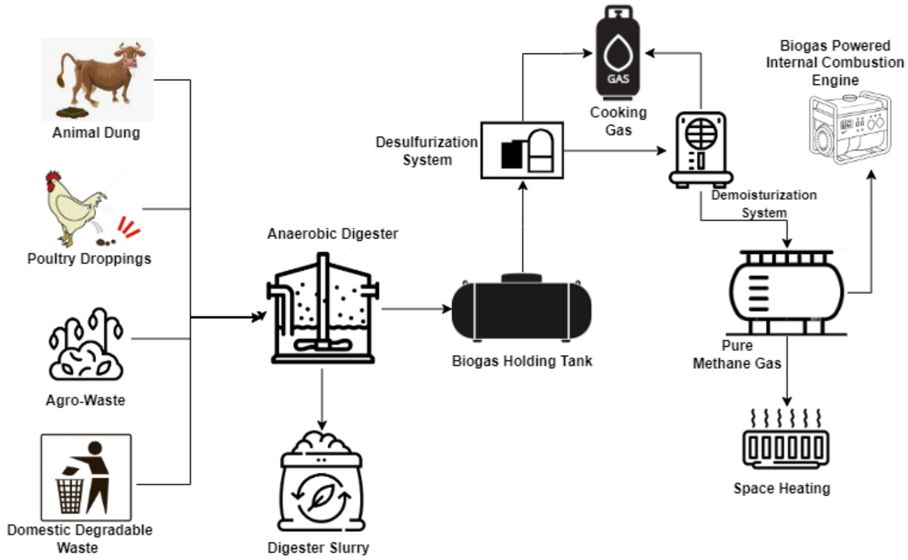

Figure 1: Digestion Framework Employed

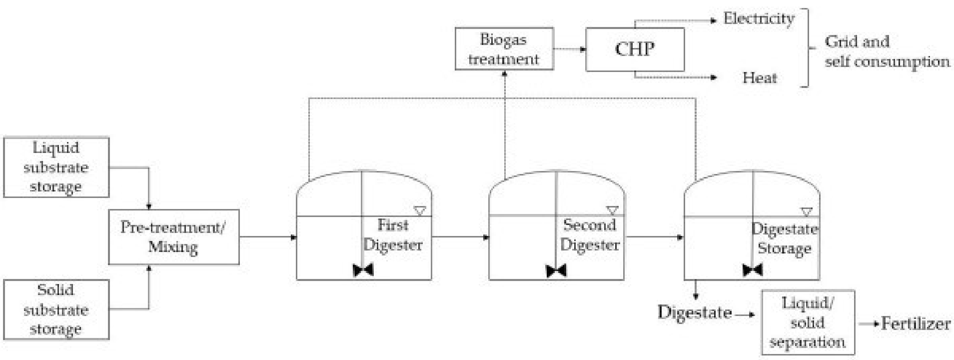

Figure 2: Overview of the Anaerobic Digestion (AD) Process

Table 1: Operating envelope and variables used for modelling (Appendix 1, n=61 days)

Variable	Unit	Min	Max	Role in study
Average working temperature	°C	28.0	40.0	ANN input: operating condition
Biogas generated	m³/day	10.0	22.0	ANN input: energy conversion
CO_2 fraction	%	11.0	35.0	ANN input: gas quality indicator
pH	–	7.2	9.6	ANN input: process stability indicator
H_2S	m³/day	0.020	0.044	ANN input: impurity indicator
ICE operating time	h/day	8.3	18.3	ANN input: electricity conversion context
Methane volume	m³/day	6.50	12.09	ANN output (target)
Electricity generated	kWh/day kWh	10.0	22.0	Energy output: performance indicator

Instrumentation and IoT data acquisition

The monitoring system combined direct sensor measurements with process and operational records. An ESP32 development board was interfaced with a waterproof digital temperature probe and a capacitive moisture sensor. Temperature was retained as a predictor in the modelling dataset, whereas moisture was used for feedstock-condition monitoring but was not included in the aligned prediction dataset. Sensor signals were sampled at fixed intervals, locally filtered, time-stamped, and transmitted through wireless communication for storage and subsequent analysis. Moisture calibration used dry and saturated references, while temperature measurements were cross-checked against a reference thermometer.

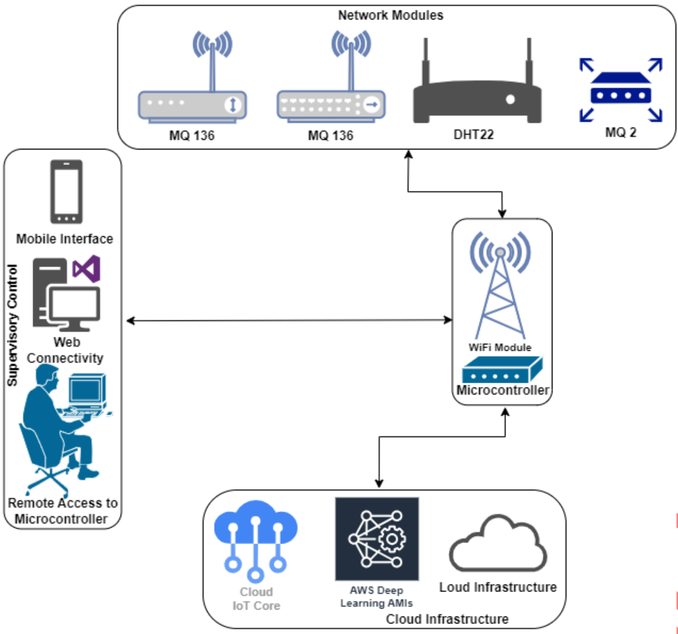

Figure 3: Sensor-Based Monitoring and Data-Flow Framework for the Developed Anaerobic Digester

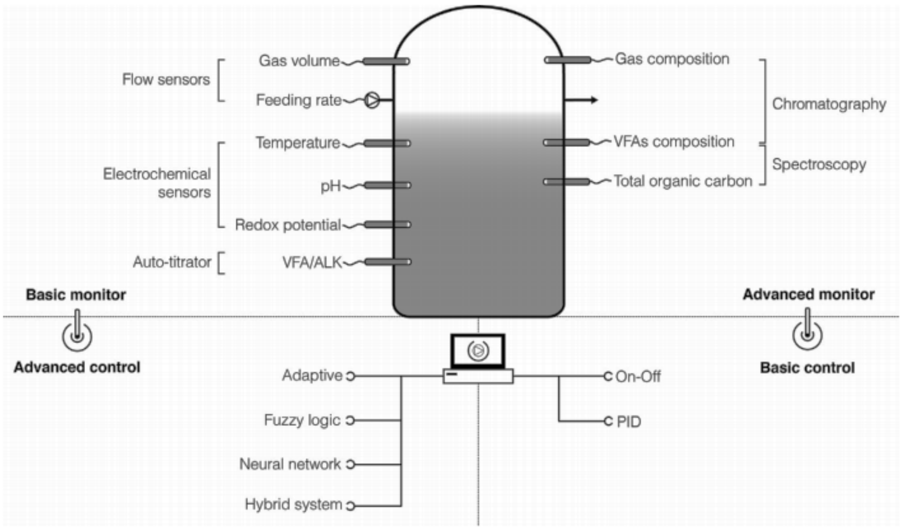

Figure 4: Conceptual Monitoring and Control Options for Anaerobic Digestion; Only Components Described in the Present Methodology Were Implemented

Table 2: IoT node specification and data pipeline

Subsystem	Implementation	Indicative cost (USD)
Controller	ESP32 development board, WROOM-32 class	10.00
Temperature sensor	Waterproof DS18B20-class probe	9.95
Moisture sensor	Capacitive analogue sensor	5.90
Sampling and communication	Embedded processing and wireless communication	Included
Core sensing-node hardware		25.85

Prices represent indicative single-unit retail values accessed in August 2026 and exclude the digester vessel, gas-treatment equipment, electricity generator, enclosure, wiring, installation, shipping, taxes, and cloud-service costs. The low-cost designation, therefore, applies specifically to the monitoring subsystem rather than the complete plant. The verified representative prices are USD 10.00 for an ESP32 development board, USD 9.95 for a waterproof DS18B20 probe, and USD 5.90 for a capacitive sensor, giving USD 25.85 for the three core components.

Gas and process measurements

Daily analytical variables comprised temperature, biogas volume, carbon dioxide fraction, pH, hydrogen sulfide, methane volume, internal combustion engine operating time, and electrical energy. Temperature represented the thermal operating condition, while moisture was retained only for feedstock monitoring. Biogas volume represented overall gas production; carbon dioxide and hydrogen sulfide characterised gas quality; pH represented process condition; and engine operating time represented generator utilisation. Methane volume was the target for prediction, while electrical energy was the final performance indicator. The variables were used for statistical association analysis, methane prediction, and energy conversion assessment. (Appendix 2).

Theoretical methane yield formulation

To provide a consistent theoretical basis for methane generation, the stoichiometric methane potential was expressed in terms of the Buswell formulation. For an organic substrate with empirical composition $C_xH_yO_z$The balanced overall reaction is shown in (1):

$$C_xH_yO_z + \left[x - \frac{y}{4} - \frac{z}{2}\right] H_2O = \left[\frac{x}{2} - \frac{y}{8} - \frac{z}{4}\right] CO_4 + \left[\frac{x}{2} + \frac{y}{8} - \frac{z}{4}\right] CO_2 \qquad (1)$$

For substrates including nitrogen and sulfur $C_xH_yO_zN_vS_u$, the extended form is in eqn. (2)

$$C_xH_yO_zN_vS_u + \left[x - \frac{y}{4} - \frac{z}{2} + \frac{3v}{4} + \frac{u}{2}\right] H_2O = \left[\frac{x}{2} - \frac{y}{8} - \frac{z}{4} - \frac{3v}{8} - \frac{u}{4}\right] CH_4$$
$$+ \left[\frac{x}{2} - \frac{y}{8} - \frac{z}{4} - \frac{3v}{8} - \frac{u}{4}\right] CO_2 + xNH_3 + yH_2S \qquad (2)$$

Equations (1) and (2) provide the theoretical stoichiometric link between feedstock elemental composition and methane generation, and are used here to frame the expected methane formation pathway during AD.

Biogas to electricity conversion

For the methane fraction and methane volume, this is given by eqn. (3) and (4)

$$xCH_4 = \frac{V_{CH_4}}{V_{BG}} \qquad (3)$$

For the chemical energy in methane, using the lower heating value (LHV) of methane at standard conditions $LVH_{CH_4} = 35.8\ \mathrm{MJ/Nm^3}$ (ISO 6976:2016), The daily chemical energy is given by the equation (4):

$$E_{chem}(\mathrm{MJ}) = V_{CH_4}(\mathrm{Nm^3}) * LHV_{CH_4}(\mathrm{MJ/Nm^3}) \qquad (4)$$

Equation (4) converted to kWh is shown in equation (5):

$$E_{chem}(\mathrm{kWh}) = \frac{E_{chem}(\mathrm{MJ})}{3.6} \qquad (5)$$

Electrical output, average electrical power, and conversion efficiency. The daily electrical energy is recorded as $E_{el}(kWh)$. The average generated electrical power across the ICE operating window is given by equation (6).

$$P_{avg}(\mathrm{kW}) = \frac{E_{el}(\mathrm{kWh})}{t_{ICE}(h)} \qquad (6)$$

Electrical conversion efficiency is given by equation (7).

$$\eta_{el} = \frac{E_{el}}{E_{CH_4}(\mathrm{kWh})} \qquad (7)$$

Control techniques, block logic, and feedback equations

Figures 3 and 4 present a proposed layered supervisory control framework that combines measured process information with predictive decision support. The hysteresis, moisture-threshold, and proportional-integral-derivative equations specify potential low-level actuation logic. However, controller performance under deliberately imposed disturbances was not experimentally evaluated. The equations (8-10) are therefore treated as control-design logic rather than experimentally validated closed-loop performance.

For temperature regulation, hysteresis control is defined around the temperature setpoint T_{set} and associated deadband ΔT, as expressed in Equation (8). The heater or insulation action $u_T \in \{0, 1\}$

$$u_T(k) = \begin{cases} 1, & T(k) < T_{set} - \Delta T \\ 0, & T(k) < T_{set} + \Delta T \\ u_T(k-1), & \text{otherwise} \end{cases} \quad (8)$$

The moisture control (threshold-based feed conditioning with moisture target M_{set} and deadband ΔM, the conditioning action $u_T \in \{0, 1\}$ is given by equation (9).

$$u_T(k) = \begin{cases} 1, & M(k) < M_{set} - \Delta T \\ 0, & M(k) < M_{set} + \Delta T \\ u_T(k-1), & \text{otherwise} \end{cases} \quad (9)$$

The general PID feedback when proportional actuation is available for any controlled output y with reference r, error $e(k) = r(k) - y(k)$, and sampling time T_s, the discrete PID law is given by the equation (10):

$$u(k) = K_p e(k) + K_i \sum_{i=0}^{k} e(i) T_s + K_d \frac{e(k) - e(k-1)}{T_s}, \quad (10)$$

Supervisory ANN-based optimisation

The ANN provides daily methane prediction as a soft-sensor signal for supervisory decision support. Its output may inform decisions on temperature, feed conditioning, and generator scheduling, but it does not directly issue actuator commands in the present study. This is presented in Table 3.

Table 3: Control blocks, feedback variable, and governing equation

Control block	Feedback variable	Control action	Equation
Temperature stabilisation	T	heater command u_T	Eq. (8) or Eq. (10)
Moisture conditioning	M	feedwater command u_M	Eq. (9)
Gas utilisation scheduling	$E_{el} t_{ICE}$	ICE runtime planning	Eq. (6), plus operational constraint

Artificial Neural Network Model Development, Training Procedure, and Validation

The ANN was developed to predict daily methane output V_{CH_4} from routinely measurable daily process variables, enabling forecast-based optimisation and improved operational decisions. The ANN structure follows a multilayer perceptron mapping:

$$h^{(1)} = f\left(W^{(1)} + b^{(1)}\right), \qquad h^{(2)} = f\left(W^{(2)} h^{(1)} + b^{(2)}\right), \qquad \hat{y} = W^{(3)} h^{(2)} + b^{(3)} \quad (11)$$

where x is the input feature vector, $f(\cdot)$ is the activation function, and $\hat{y}$ is the predicted methane volume. The vector x included $[T, V_{BC}, CO_2, pH, H_2S, t_{ICE}]$, and the output y was the daily methane volume V_{CH_4} (Appendix 2). For preprocessing, all numeric inputs were standardised using z-score scaling to avoid dominance by variables with larger magnitudes. Outliers were retained because they represent operational variability relevant to decentralised AD, but model robustness was assessed through residual analysis (Figures 8 and 9).

The validation test split and the training dataset (n = 61) were randomly split into 70% training, 15% validation, and 15% testing, with a fixed random seed for reproducibility. The ANN used two hidden layers with logistic activation and a linear output layer. Training used an adaptive gradient-based optimiser (Adam class) with early stopping when the validation loss ceased improving. The reproducible configuration for the ANN architecture and training settings is shown in Table 4. The 6-12-8-1 architecture was selected as a compact nonlinear configuration that represents interactions among the six predictors while limiting model complexity on the relatively small dataset. To determine whether nonlinear model complexity was justified, multiple linear regression was developed as a baseline using the same six predictors and the same fixed 70/15/15 data allocation. Both models were evaluated using identical error and goodness-of-fit measures.

Table 4: ANN architecture and training settings

Item	Specification
Inputs	6 features $[T, V_{BC}, CO_2, pH, H_2S, t_{ICE}]$,
Output	Methane volume V_{CH_4}
Architecture	6–12–8–1 (two hidden layers: 12 and 8 neurons)
Activation	Logistic in hidden layers; linear output
Optimiser	Adam class, learning rate 0.001
Regularisation	L2 penalty $\alpha = 1 \times 10^{-4}$
Stopping	Early stopping, patience 50 iterations, max iterations 10,000
Split	70/15/15 (train/validation/test), fixed seed

For the error metrics and validation plots, the model accuracy was quantified using RMSE, MAE, coefficient of determination R^2, and MAPE is given by equation (12):

$$RMSE = \sqrt{\frac{1}{n}\sum_{i=1}^{n}(y_i - \hat{y}_i)^2}, \quad MAE = \frac{1}{n}\sum_{i=1}^{n}|y_i - \hat{y}_i|, \quad MAPE = \frac{100}{n}\sum_{n=1}^{n}\left|\frac{y_i - \hat{y}_i}{y_i}\right| \quad (12)$$

A parity plot (predicted vs measured) and a residual plot were used for visual validation, as shown in Figures 8 and 9. Predictive performance is summarised in Table 5, while Figures 8 and 9 provide parity and residual assessments for the neural-network predictions.

Table 5: Predictive Performance and Linear Baseline Comparison

Dataset/Model	RMSE (m³/day)	MAE (m³/day)	R^2	MAPE (%)
Neural network, training	0.465	0.363	0.895	3.34
Neural network, validation	0.616	0.487	0.802	5.26
Neural network, test	0.593	0.458	0.856	5.06
Multiple linear regression, test	0.416	0.265	0.929	3.26

Statistical analysis

Pairwise linear associations among variables were quantified using the Pearson correlation coefficient, which is given in equations (13) and (14):

$$r = \frac{\sum_{i=1}^{n}(x_i - \bar{x})(y_i - \bar{y})}{\sqrt{\sum_{i=1}^{n}(x_i - \bar{x})^2}\,\sqrt{\sum_{i=1}^{n}(y_i - \bar{y})}} \quad (13)$$

The statistical significance of correlations was assessed using:

$$t = r\sqrt{\frac{n-2}{1-r^2}}, \qquad df = n - 2 \quad (14)$$

Variance inflation factor analysis was additionally used to assess predictor collinearity. Severe multicollinearity was identified among temperature, biogas volume, carbon dioxide, pH, and hydrogen sulfide because these variables were subject to the same controlled operating profile. Consequently, the correlation coefficients and individual predictor relationships were interpreted descriptively rather than as independent causal effects.

RESULTS

Daily operation showed a ramp-up, seven-day plateau, and subsequent ramp-down across the investigated operating profile. Reactor temperature ranged from 28.0°C to 40.0°C, methane output from 6.50 to 12.09 m³/day, and daily electrical energy from 10.0 to 22.0 kWh, while the carbon dioxide fraction ranged from 35% to 11%. The seven-day peak condition occurred from 07 to 13 February 2024 at 40°C, with methane and electrical energy reaching 12.09 m³/day and 22.0 kWh, respectively. The regular trajectory reflects the hybrid dataset, which combines monitored observations with controlled-profile augmentation. It therefore characterises the investigated operating envelope rather than 61 fully independent experimental responses.

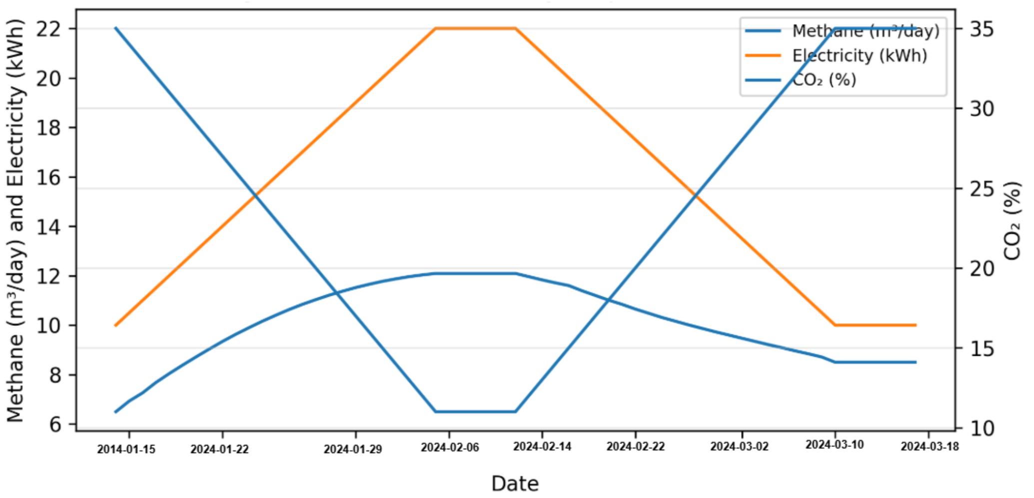

Figure 5: Daily methane and electricity output (left axis) with CO_2 trend (right axis) over the monitoring window

Using the methane volumes represented in the hybrid dataset and the lower heating value stated in the methodology, the implied electrical conversion efficiency ranged from 11.8% to 18.3%, with a mean of 15.5%. Based on daily electricity and ICE operating hours, the average electrical power delivered during engine operation ranged from 0.93 to 1.23 kW (mean 1.14 kW), supporting the feasibility of low-power decentralised supply from waste-derived biogas under the tested conditions.

Figure 6 shows strong associations among the operating variables and electrical output. Near-perfect correlations are observed for temperature, biogas volume, pH, hydrogen sulfide, and carbon dioxide because these variables covary with the structured operating profile. Methane volume and engine operating time are also strongly associated with electrical output. These coefficients therefore describe common variation within the investigated dataset and should not be interpreted as independent causal effects. The severe collinearity further limits the interpretation of individual predictor importance.

Year 2026
Volume 2, Issue 4, 1030777

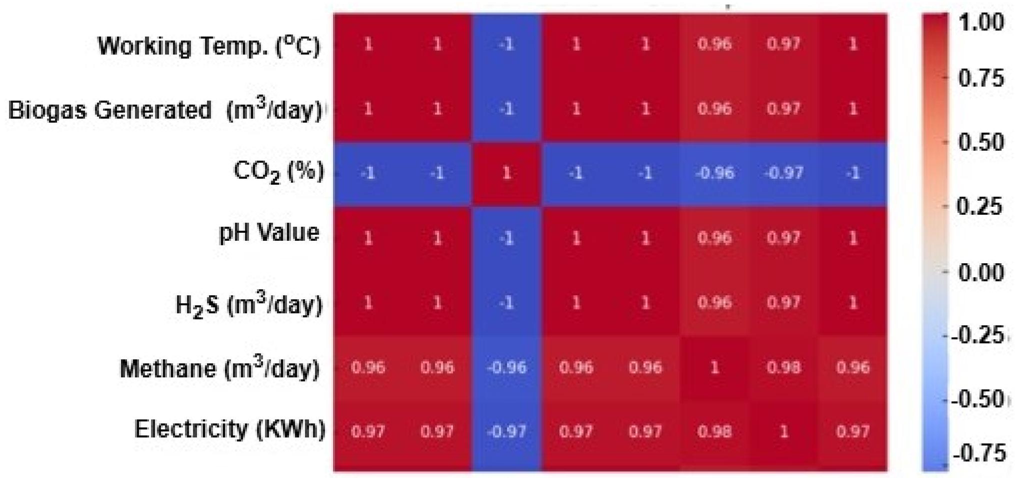

Figure 6: Pearson correlation heatmap for daily operating parameters, gas constituents, and electricity output (n = 61 days).

Figure 7 illustrates the 6-12-8-1 neural-network architecture used to predict methane output from temperature, biogas volume, carbon dioxide, pH, hydrogen sulfide, and engine operating time. Predictive usefulness was assessed from held-out performance and direct comparison with the linear-regression baseline rather than from network complexity alone.

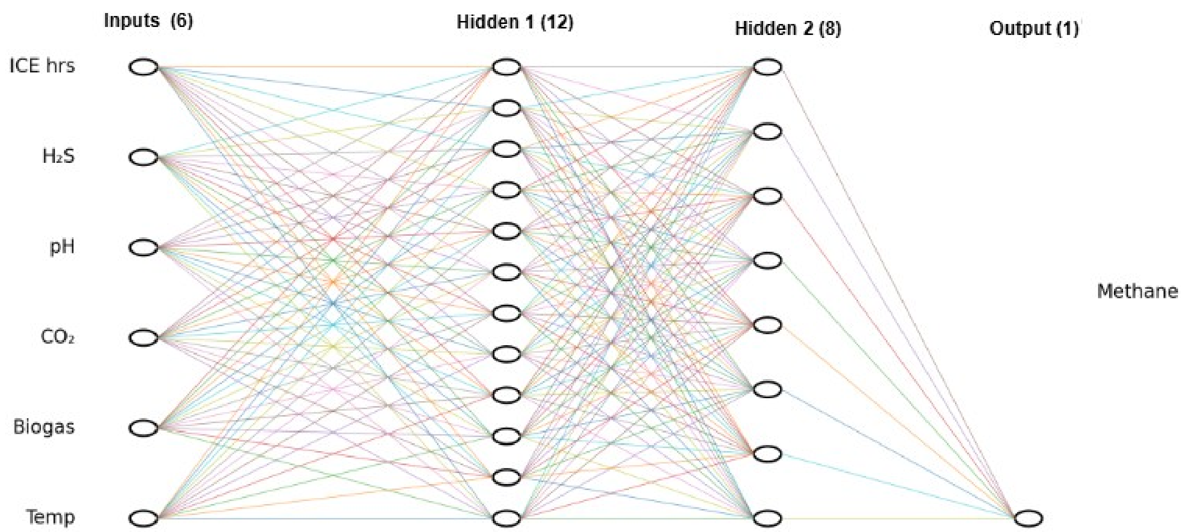

Figure 7: Artificial Neural Network Architecture Used for Methane Prediction

On the test set, the artificial neural network achieved RMSE = 0.593 m³/day, MAE = 0.458 m³/day, $R^2 = 0.856$, and MAPE = 5.06%. Multiple linear regression achieved RMSE = 0.416 m³/day, MAE = 0.265 m³/day, $R^2 = 0.929$, and MAPE = 3.26%. The simpler linear model, therefore, performed better on the present structured dataset. The neural network demonstrates predictive feasibility within the investigated operating range but provides no evidence of superior predictive accuracy. Figures 8 and 9 should consequently be interpreted as validation of neural-network behaviour within the evaluated split rather than evidence of unrestricted generalisability.

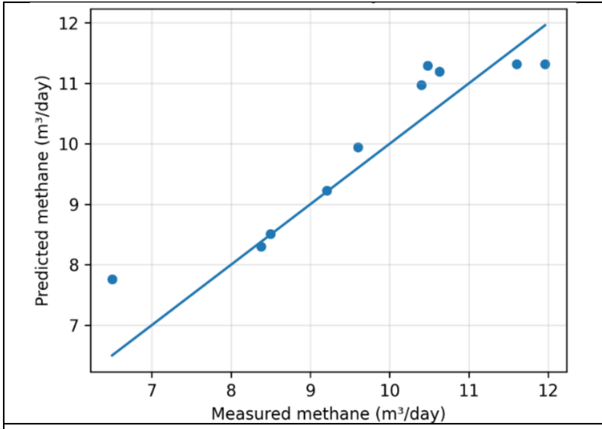

Figure 8: Predicted versus measured methane output (test set parity plot)

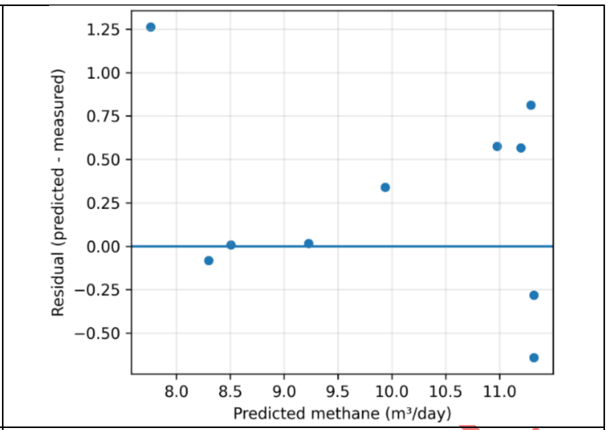

Figure 9: Residuals (predicted − measured methane) versus predicted methane output for the test set.

The demonstrated biogas-to-electricity pathway is consistent with renewable-energy and resource-recovery objectives represented by Sustainable Development Goals 7 and 12. However, the hybrid dataset, the lack of row-level separation of measured and augmented observations, strong predictor collinearity, and the absence of closed-loop disturbance testing limit broader interpretation. Future work should therefore evaluate the framework using independently measured data under variable feed, loading, temperature, and gas-quality conditions, together with experimental controller validation.

CONCLUSION

This study demonstrated an anaerobic digestion electricity-generation framework that integrates low-cost sensor-based monitoring, methane prediction, and energy performance assessment. Across the investigated operating envelope, methane output ranged from 6.50 to 12.09 m^3/day and daily electrical energy from 10.0 to 22.0 kWh, with an implied electrical conversion efficiency of 11.8% to 18.3% and a mean of 15.5%. The artificial neural network achieved a test R^2 of 0.856 and MAPE of 5.06%; however, multiple linear regression achieved a higher R^2 of 0.929 and lower MAPE of 3.26%, indicating that additional nonlinear complexity was not advantageous for the structured dataset. The principal contribution is therefore the integrated sensing, energy accounting, model benchmarking, and supervisory framework rather than neural-network superiority. Further validation using independently measured, more variable operating data and experimentally tested closed-loop control is required before broader deployment claims can be made.

ACKNOWLEDGMENT(S)

The authors would like to acknowledge the First Technical University, Ibadan, Nigeria, for providing the facilities used to conduct this research.

REFERENCES

[1] H. Seyedhashemi, B. Hingray, C. Lavaysse, and T. Chamarande, “The Impact of Low-Resource Periods on the Reliability of Wind Power Systems for Rural Electrification in Africa,” *Energies*, vol. 14, no. 11, p. 2978, 2021, doi: 10.3390/en14112978.

[2] Telukhunoana, M. M., Kali, M., & Lemaire, X. (2026). Community-driven approaches to rural electrification: insights and lessons from Lesotho. *SN Social Sciences*, *6*(2), 54. doi: 10.1007/s43545-025-01219.

[3] Coban, H. H. (2024). A multiscale approach to optimize off-grid hybrid renewable energy systems for sustainable rural electrification: economic evaluation and design. *Energy Strategy Reviews*, 55, 101527. doi: 10.1016/j.esr.2024.101527.

[4] Lwakatare, B., Vyavahare, P., Mehta, K., & Zörner, W. (2024). Electrification planning for off-grid communities in Sub-Saharan Africa: Advancing energy access. *Energies*. i, 17(23), 5994. doi: 10.3390/en17235994.

[5] Gyimah, J., Liu, Y., Nyantakyi, G., & Yao, X. (2024). The effect of mini‐grid rural electrification on urbanization: Evidence from the pilot mini‐grid systems in Ghana. *Review of Development Economics*, 28(3), 1108-1130.3. doi: 10.1111/rode.13093.

[6] Effiong, I., Anandarajah, G., & Dessens, O. (2026). The Impact of Mini-Grids on Rural Energy-Access Indicators in Developing Countries: A Systematic Review. *Energies*, 19(6), 1441.

[7] Bhanye, J., Kloeffel, T., Beyers, M., Mabaso, M., Rajadurai, K., Winklmaier, J., & Matamanda, A. (2024). Decentralised water–energy–food (WEF) systems in Africa: space analysis, least-cost modelling of sack farming and establishment of renewable energy technologies in the Diepsloot slums of Johannesburg, South Africa. Discover Global Society, 2(1), 24. doi: 10.1007/s44282-024-00052-w.

[8] K. M. Nyarko, J. Whale, and T. Urmee, "Drivers and Challenges of Off-Grid Renewable Energy-Based Projects in West Africa: A Review," *Heliyon*, vol. 9, no. 6, p. e16710, 2023, doi: 10.1016/j.heliyon.2023.e16710.

[9] Rasimphi, T., Kilonzo, B., Tjale, M., Tinarwo, D., & Nyamukondiwa, P. (2024). Review of implementation of biogas technology in rural communities of South Africa. *Cogent Social Sciences*, 10(1), 2419536.

[10] N. Yimen *et al.*, "Optimal Sizing and Techno-Economic Analysis of Hybrid Renewable Energy Systems—A Case Study of a Photovoltaic/Wind/Battery/Diesel System in Fanisau, Northern Nigeria," *Processes*, vol. 8, no. 11, p. 1381, 2020, doi: 10.3390/pr8111381.

[11] F. Antoñanzas-Torres, J. Antonanzas, and J. Blanco-Fernández, "State-of-the-Art of Mini Grids for Rural Electrification in West Africa," *Energies*, vol. 14, no. 4, p. 990, 2021, doi: 10.3390/en14040990.

[12] Richard, L., Saincy, N., Le Saux, N., Frey, D., Alvarez-Herault, M. C., & Raison, B. (2023). A New Electrification Model to End Energy Poverty: An example from a novel rural electrification approach in Madagascar. *IEEE Electrification Magazine*, 11(2), 62-73.

[13] M. Grimm, L. Lenz, J. Peters, and M. Sievert, "Demand for Off-Grid Solar Electricity: Experimental Evidence From Rwanda," *J. Assoc. Environ. Resour. Econ.*, vol. 7, no. 3, pp. 417–454, 2020, doi: 10.1086/707384.

[14] A. Korzhenevych and C. K. Owusu, "Renewable Minigrid Electrification in Off-Grid Rural Ghana: Exploring Households Willingness to Pay," *Sustainability*, vol. 13, no. 21, p. 11711, 2021, doi: 10.3390/su132111711.

[15] C. S. Segura-Salas, K. A. e. Silva, A. M. de M. Goncalves, and H. H. S. do Nascimento, "Off-Grid Photovoltaic Systems Implementation for Electrification of Remote Areas: Experiences and Lessons Learned in the Pantanal Sul-Mato-Grossense Region of Brazil," *Brazilian Arch. Biol. Technol.*, vol. 66, 2023, doi: 10.1590/1678-4324-2023210482.

[16] D. Sahara, "Livestock Waste as Alternative Energy for Rural Households: A Review," *Iop Conf. Ser. Earth Environ. Sci.*, vol. 1292, no. 1, p. 12002, 2024, doi: 10.1088/1755-1315/1292/1/012002.

[17] C. Bux, "Biomethane and Compost Production by Anaerobic Digestion of Organic Waste: Suggestions for Rural Communities in Southern Italy," *Sustainability*, vol. 15, no. 21, p. 15644, 2023, doi: 10.3390/su152115644.

[18] E. Rahmawati, Mujianto, A. Amir, T. D. Sukarno, and Супрапеди, "Rural Waste Management Model in Creating an Inclusive Economy," *Iop Conf. Ser. Earth Environ. Sci.*, vol. 1180, no. 1, p. 12005, 2023, doi: 10.1088/1755-1315/1180/1/012005.

[19] J. M. Masjhoer, S. Syafrudin, and M. Maryono, "Household and Household-Related

Waste Generation and Characteristics in Rural Areas: A Case Study in Tanjungsari Sub-District," *Sustinere J. Environ. Sustain.*, vol. 6, no. 3, pp. 174–184, 2023, doi: 10.22515/sustinerejes.v6i3.246.

[20] Wilson, D. C., Paul, J., Ramola, A., & Filho, C. S. (2024). Unlocking the significant worldwide potential of better waste and resource management for climate mitigation: with particular focus on the Global South. Waste Management & Research, 42(10), 860-872.

[21] K. O. Olatunji, N. A. Ahmed, and O. Ogunkunle, "Optimization of biogas yield from lignocellulosic materials with different pretreatment methods: a review," *Biotechnol. Biofuels*, vol. 14, no. 1, p. 159, 2021, doi: 10.1186/s13068-021-02012-x.

[22] D. Thakur, S. Kumar, V. Kumar, and T. Kaur, "Estimation of calorific value using an artificial neural network based on stochastic ultimate analysis," *Renew. Energy*, vol. 228, p. 120668, 2024.

[23] Uddin, M. M., & Wright, M. M. (2023). Anaerobic digestion fundamentals, challenges, and technological advances. *Physical Sciences Reviews*, 8(9), 2819-2837.

[24] Swami, S., Suthar, S., Singh, R., Thakur, A. K., Gupta, L. R., & Sikarwar, V. S. (2025). Integration of anaerobic digestion with artificial intelligence to optimise biogas plant operation. *Environment, Development and Sustainability*, 27(5), 9773-9803.

[25] B. Yang, Q. Yu, and Y. Zhang, "Applying Dynamic Magnetic Field to Promote Anaerobic Digestion via Enhancing the Electron Transfer of a Microbial Respiration Chain," *Environ. Sci. Technol.*, vol. 57, no. 5, pp. 2138–2148, 2023, doi: 10.1021/acs.est.2c08577.

[26] I. Juárez-Barojas, R. Posada-Gómez, A. Alvarado-Lassman, and J. P. Rodríguez-Jarquín, "Condition-Based Maintenance of an Anaerobic Reactor Using Artificial Intelligence," *Electronics*, vol. 12, no. 4, p. 799, 2023.

[27] J. J. Coêlho, A. Hennessy, I. A. Casey, T. Woodcock, and N. Kennedy, "Biofertilisation With Anaerobic Digestates: Effects on the Productive Traits of Ryegrass and Soil Nutrients," *J. Soil Sci. Plant Nutr.*, vol. 20, no. 4, pp. 1665–1678, 2020, doi: 10.1007/s42729-020-00237-7.

[28] F. Aweenagua, J. Takyi, M. N. V Williams, F. A. Gatsi, and H. R. Beem, "Design and Implementation of an IoT-based Smart Household Biogas Digester," in *2024 IST-Africa Conference (IST-Africa)*, IEEE, 2024, pp. 1–9.

[29] T. D. d. Santos, E. de A. do Couto, and E. M. Vieira, "Mapping the Potential of the State of Minas Gerais, Brazil, in Generating Electricity From Biogas From Anaerobic Digestion of Vinasse," *Rev. Bras. Gestão Ambient. E Sustentabilidade*, vol. 8, no. 19, pp. 793–801, 2021, doi: 10.21438/rbgas(2021)081909.

[30] Z. Li, X. Zhou, X. Wang, and S. Zuo, "Anaerobic Co-Digestion of Kitchen Waste and Blackwater for Different Practical Application Scenarios in Decentralized Scale: From Wastes to Energy Recovery," *Water*, vol. 12, no. 9, p. 2556, 2020, doi: 10.3390/w12092556.

[31] Ugwu, S. N., Harding, K., & Enweremadu, C. C. (2022). Comparative life cycle assessment of enhanced anaerobic digestion of agro-industrial waste for biogas production. *Journal of Cleaner Production*, 345, 131178.

[32] K. Obileke, N. Nwokolo, G. Makaka, P. Mukumba, and H. Onyeaka, "Anaerobic Digestion: Technology for Biogas Production as a Source of Renewable Energy—A Review," *Energy Environ.*, vol. 32, no. 2, pp. 191–225, 2020, doi: 10.1177/0958305x20923117.

[33] M.-F. Shih, C. Lin, and C.-H. Lay, "Comparison of Potential Environmental Impacts and Waste-to-Energy Efficiency for Kitchen Waste Treatment Scenarios in Central Taiwan," *Processes*, vol. 9, no. 4, p. 696, 2021, doi: 10.3390/pr9040696.

[34] Lu, X., Liu, Y., Gao, Y., Liu, Z., Sun, Y., Li, J., ... & Zhen, G. (2025). Feasibility of In Situ Bioelectrocatalytic Computation to Implement Simultaneous Nitrogen Removal of

Anaerobic Digestate and Biogas Upgrading. *ACS ES&T Water*, 5(3), 1331-1343.
[35] J. Jamaluddin and Z. Zulkeflee, "Co-Digestion of Water Hyacinth and Duck Manure for Potential Low-Cost Biogas Production by Rural Communities," *Clean - Soil Air Water*, 2023, doi: 10.1002/clen.202200127.
[36] B. Steiniger, C. Hubert, and C. Schaum, "Digesters as Heat Storage: Effects of the Digester Temperature on the Process Stability, Sludge Liquor Quality, and the Dewaterability," *Water Environ. Res.*, 2023, doi: 10.1002/wer.10918.

APPENDIX

Appendix 1: Anaerobic Digester Output Data

Date of Operation	Average Working Temp. (°C)	Biogas Generated (m^3/day)	CO_2 (%)	pH Value	H_2S (m^3/day)	Methane (m^3/day)	ICE Operating (Hrs)	Electricity Generated (kWh)
14/01/2024	28	10	35	7.2	0.02	6.5	8.3	10
15/01/2024	28.5	10.5	34	7.3	0.021	6.93	8.8	10.5
16/01/2024	29	11	33	7.4	0.022	7.26	9.2	11
17/01/2024	29.5	11.5	32	7.5	0.023	7.68	9.6	11.5
18/01/2024	30	12	31	7.6	0.024	8.04	10	12
19/01/2024	30.5	12.5	30	7.7	0.025	8.38	10.4	12.5
20/01/2024	31	13	29	7.8	0.026	8.71	10.8	13
21/01/2024	31.5	13.5	28	7.9	0.027	9.03	11.3	13.5
22/01/2024	32	14	27	8	0.028	9.34	11.7	14
23/01/2024	32.5	14.5	26	8.1	0.029	9.63	12.1	14.5
24/01/2024	33	15	25	8.2	0.03	9.9	12.5	15
25/01/2024	33.5	15.5	24	8.3	0.031	10.16	12.9	15.5
26/01/2024	34	16	23	8.4	0.032	10.4	13.3	16
27/01/2024	34.5	16.5	22	8.5	0.033	10.63	13.8	16.5
28/01/2024	35	17	21	8.6	0.034	10.84	14.2	17
29/01/2024	35.5	17.5	20	8.7	0.035	11.03	14.6	17.5
30/01/2024	36	18	19	8.8	0.036	11.21	15	18
31/01/2024	36.5	18.5	18	8.9	0.037	11.37	15.4	18.5
01/02/2024	37	19	17	9	0.038	11.52	15.8	19
02/02/2024	37.5	19.5	16	9.1	0.039	11.65	16.3	19.5
03/02/2024	38	20	15	9.2	0.04	11.77	16.7	20
04/02/2024	38.5	20.5	14	9.3	0.041	11.87	17.1	20.5
05/02/2024	39	21	13	9.4	0.042	11.96	17.5	21
06/02/2024	39.5	21.5	12	9.5	0.043	12.03	17.9	21.5
07/02/2024	40	22	11	9.6	0.044	12.09	18.3	22
08/02/2024	40	22	11	9.6	0.044	12.09	18.3	22
09/02/2024	40	22	11	9.6	0.044	12.09	18.3	22
10/02/2024	40	22	11	9.6	0.044	12.09	18.3	22
11/02/2024	40	22	11	9.6	0.044	12.09	18.3	22
12/02/2024	40	22	11	9.6	0.044	12.09	18.3	22
13/02/2024	40	22	11	9.6	0.044	12.09	18.3	22
14/02/2024	39.5	21.5	12	9.5	0.043	11.96	17.5	21.5
15/02/2024	39	21	13	9.4	0.042	11.83	17.2	21
16/02/2024	38.5	20.5	14	9.3	0.041	11.71	16.9	20.5
17/02/2024	38	20	15	9.2	0.04	11.6	16.6	20
18/02/2024	37.5	19.5	16	9.1	0.039	11.39	16.3	19.5
19/02/2024	37	19	17	9	0.038	11.2	16	19
20/02/2024	36.5	18.5	18	8.9	0.037	11.01	15.7	18.5
21/02/2024	36	18	19	8.8	0.036	10.84	15.5	18
22/02/2024	35.5	17.5	20	8.7	0.035	10.65	15.2	17.5
23/02/2024	35	17	21	8.6	0.034	10.48	14.9	17
24/02/2024	34.5	16.5	22	8.5	0.033	10.31	14.6	16.5
25/02/2024	34	16	23	8.4	0.032	10.16	14.3	16
26/02/2024	33.5	15.5	24	8.3	0.031	10.01	14	15.5
27/02/2024	33	15	25	8.2	0.03	9.87	13.7	15
28/02/2024	32.5	14.5	26	8.1	0.029	9.73	13.4	14.5
29/02/2024	32	14	27	8	0.028	9.6	13.1	14

01/03/2024	31.5	13.5	28	7.9	0.027	9.47	12.8	13.5
02/03/2024	31	13	29	7.8	0.026	9.34	12.5	13
03/03/2024	30.5	12.5	30	7.7	0.025	9.21	12.2	12.5
04/03/2024	30	12	31	7.6	0.024	9.09	11.9	12
05/03/2024	29.5	11.5	32	7.5	0.023	8.96	11.6	11.5
06/03/2024	29	11	33	7.4	0.022	8.84	11.3	11
07/03/2024	28.5	10.5	34	7.3	0.021	8.71	11	10.5
08/03/2024	28	10	35	7.2	0.02	8.5	10.7	10
09/03/2024	28	10	35	7.2	0.02	8.5	10.7	10
10/03/2024	28	10	35	7.2	0.02	8.5	10.7	10
11/03/2024	28	10	35	7.2	0.02	8.5	10.7	10
12/03/2024	28	10	35	7.2	0.02	8.5	10.7	10
13/03/2024	28	10	35	7.2	0.02	8.5	10.7	10
14/03/2024	28	10	35	7.2	0.02	8.5	10.7	10

Appendix 2: Constituents of Output/Generated Biogas

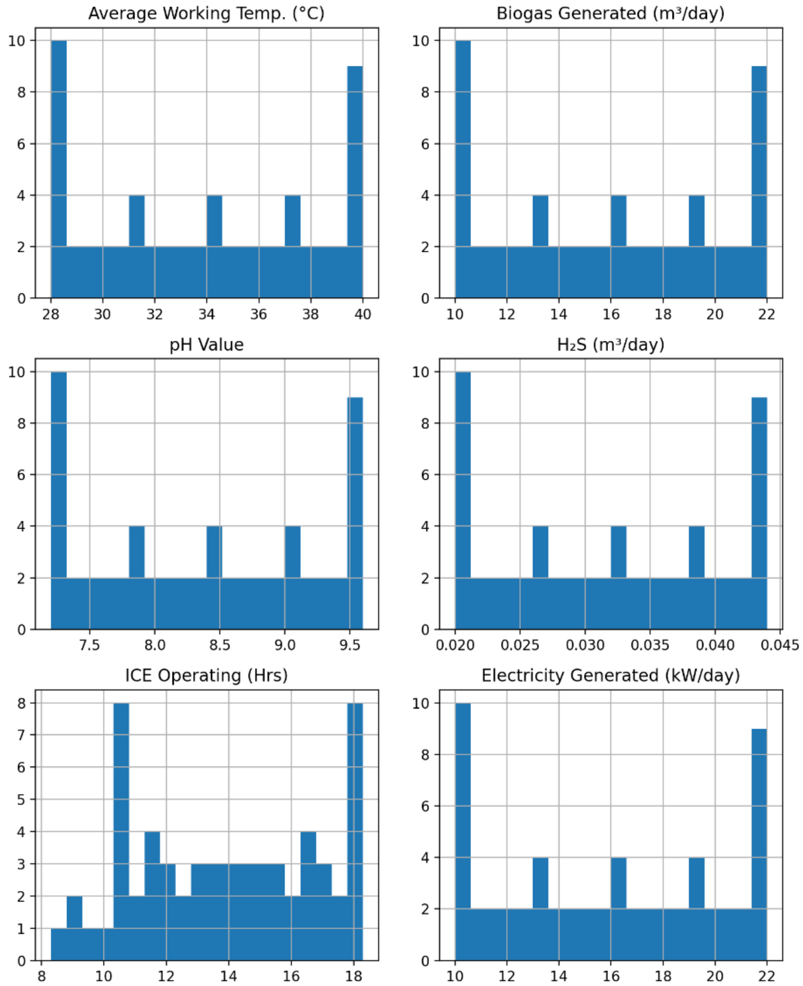

Constituents of Output/Generated Biogas

1. Methane fraction (per "gas composition" block)

$$x_{CH_4} = \frac{V_{CH_4}}{V_{biogas}} = \frac{8.04}{12} = 0.67 \approx 67\%$$

2. Chemical energy produced in methane (per "biogas energy" block)

$$E_{CH_4}(\text{MJ}) = V_{CH_4} \times LHV_{CH_4} = 8.04 \times 35.8 = 287.8\ \text{MJ}$$

3. Converting the methane chemical energy to kWh (for that day)

Year 2026
Volume 2, Issue 4, 1030777

$$E_{CH_4}(\text{kWh}) = \frac{E_{CH_4}}{3.6} = \frac{287.8}{3.6} = 80.0\ \text{kWh}$$

4. Electrical output and average generator power during operation

$$E_{el} = 12.0\ \text{kWh},\ P_{avg} = \frac{E_{el}}{t_{ICE}} = \frac{12.0}{10.0} = 1.20\ \text{kW}$$

5. Overall electricity conversion efficiency (daily)

$$\eta_{el} = \frac{E_{el}}{E_{CH_4}(\text{kWh})} = \frac{12.0}{80.0} = 0.150 \approx 15.0\%$$